REVIEWS OF GEOPHYSICS AND SPACE PHYSICS, VOL. 18, NO. 1, PAGES 203–209, FEBRUARY 1980

Geomagnetic Depth Sounding by Induction Arrow Representation: A Review

G. P. GREGORI

Istituto di Fisica dell'Atmosfera, Consiglio Nazionale delle Ricerche, 00144 Rome, Italy

L. J. LANZEROTTI

Bell Laboratories, Murray Hill, New Jersey 07974

Considerable important research in upper atmosphere geophysics is carried out through the use of arrays of ground-based magnetometers. In order to better delineate the ionospheric and magnetospheric currents and waves as measured by these arrays, it is important to understand the conductivity of the earth's structure under the individual stations. Geomagnetic depth sounding studies are used to deduce the earth's conductivity profiles. In most studies, 'induction arrows,' or 'induction vectors,' are plotted on maps for graphical representations of lateral inhomogeneities in underground conductivity structures. Different methodologies and different arrow conventions have been used by a number of authors for deriving these vectors, often without relating their techniques to other work in the field. We review herein the various methodologies (except transfer functions) and present a unifying picture to the representations that should prove useful to researchers in both space physics and solid earth physics.

INTRODUCTION

Ground-based magnetic recordings at a given site provide a measure versus time (t) of the geomagnetic field vector $\mathbf{B}(t)$ with component $H(t)$ (south-north oriented), $D(t)$ (east-west oriented), and $Z(t)$ (downward oriented in the northern hemisphere). Geomagneticians use data from arrays of magnetic stations to derive information on the electric currents flowing both in the magnetosphere/ionosphere and in the earth. It is important to understand the earth's conductivity structure under a magnetometer array in order to derive ionosphere/magnetosphere information. Thus researchers concerned with purely space-related problems must have some awareness of the earth's geologic structure.

There are three distinct problems associated with studies of ground-based geomagnetic data. These are (1) the problem of the separation of the external ($\mathbf{B}_e(t)$) and the internal ($\mathbf{B}_i(t)$) origin fields, (2) the inversion problem for $\mathbf{B}_e(t)$, and (3) the inversion problem for $\mathbf{B}_i(t)$. The first problem has been shown to have a unique solution by *Gauss* [1838] and by *Vestine* [1941]. The second problem was shown by *Fukushima* [1969, 1972] not to have a unique solution in terms of either ionosphere currents or of magnetic-field-aligned currents. The third problem can have a unique solution for special, idealized models of the earth's conductivity structure [*Bailey*, 1970; *Weidelt*, 1972]; this problem has no unique solution for the case of the actual earth.

Geomagnetic depth sounding (GDS) is the term that describes the study of underground conductivity structures using purely geomagnetic measurements. GDS is concerned solely with the first problem (above) and not with the third (as is sometimes confused in the literature). With this realization we can determine what GDS depicts concerning underground conductivity structures.

An external magnetic field with a period T will penetrate the earth to a depth where the conductivity will appear infinite at the period in question. A magnetometer on the earth's surface will record a field of period T, $\mathbf{B}_T(t)$ that is plane polarized in a plane tangent to the conductivity surface below the observing point. This plane of polarization is frequently referred to as the Parkinson plane.

The concept of GDS is schematically illustrated in Figure 1. Note that while GDS can give the orientation of the Parkinson plane, it cannot provide any information on the depth of the 'infinite' (for the period T in question) underground conductor (which would be a solution to the third problem). By examining the Parkinson planes for several different period geomagnetic variations, a qualitative notion of the distribution with depth of changes in the conductivity profiles can be obtained (a shorter-period external signal will penetrate to a more shallow depth than a longer-period signal).

'Induction vectors,' or 'induction arrows,' are vectors that help to visualize graphically on a map the orientation and qualitative intensity of an underground conductivity anomaly. A number of different techniques have been proposed in the past for deriving induction vectors. The first two of these were introduced almost simultaneously by *Parkinson* [1962*a*] and by *Wiese* [1962]. Subsequently, other vectors and techniques have been introduced by other authors. We discuss herein several different methods and vectors that have been used and show the interrelationships between the representations.

Two methods that have been used for induction vector work and that are not reviewed herein are the 'transfer function' procedure [*Schmucker*, 1964, 1970*a*, *b*; *Everett and Hyndman*, 1967] and the 'additive-criteria' [*Fanselau*, 1968*a*, *b*, 1970; *Ritter*, 1975; *Babour et al.*, 1976; *Babour and Mosnier*, 1977] using a fixed 'base' measurement station. In several nations in recent years the transfer function technique has come to supplant other methods for deriving induction vectors. However, the simplicities in several of the other approaches to induction arrow representation still attract many researchers conducting global and regional geomagnetic investigations [e.g., *Berdichevskiy et al.*, 1976; *Yamashita and Yokoyama*, 1976]. The different methodologies used by the different advocates are usually employed without relating the particular technique used to other work in the field. We show, in this review, that there is a unifying picture to the various techniques.

Paper number 9R1208.
0034-6853/80/009R-1208$06.00

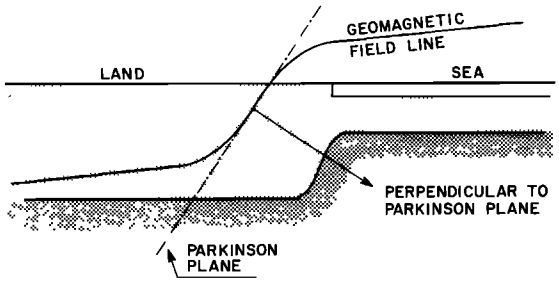

Fig. 1. Schematic illustration of earth conductivity layers. Telluric currents flowing in the deep conductivity structures (heavy grey layer in the figure) tilt the polarization plane of the observed geomagnetic field.

This unification should make such techniques of even greater utility for GDS studies and for space physics researchers than they have been heretofore.

In general, various techniques are used for decomposing the measured magnetic field $\mathbf{B}(t)$ into its various frequency components prior to determining the induction vectors. For example, selecting 'baylike' events of some given total time duration for analysis is a visual method of crudely filtering a specific frequency band. One of the most straightforward of these techniques is what we call the 'Parkinson filter,' whereby the data are sampled at fixed time intervals Δt. The filtered output is given by

$$\mathbf{W}(t, \Delta t) = \mathbf{B}(t + \Delta t) - \mathbf{B}(t) \tag{1}$$

where $\mathbf{B}(t)$ is the measured geomagnetic field with components $H(t)$, $D(t)$, and $Z(t)$. Alternative filtering procedures include decomposition into frequency components by Fourier series or by Fourier transform analysis.

Early work in New Zealand and Australia by *Baird* [1927] and by *Skey* [1928] suggested that their acquired magnetic data in the D-Z plane were linearly polarized, although in different directions depending upon the measurement site. (In terms of present-day understanding, these authors were actually studying, at each site, the intersection of the D-Z plane with the Parkinson plane.) *Bossolasco* [1936] appears to have been the first to point out specifically the plane polarization nature of the magnetic field orientation. He studied three magnetic bay events recorded in Mogadiscio, Somalia, and concluded that the perturbation field appeared to be plane polarized and that the polarization plane was independent of the intensity of the perturbation. However, he also stated that the polarization plane appeared to change with time; this was undoubtedly a result of the fact that he was using, in effect, a visual filter technique.

Rikitake and Yokoyama [1953] appear to have been the first to explicitly state mathematically the relationship between the vertical component of the field and the horizontal components:

$$Z = rH + yD \tag{2}$$

where we call r and y the Rikitake-Yokoyama constants and (2) the Rikitake-Yokoyama relationship. This formulation of the relationship is the fundamental one for use in all subsequent geometrical definitions. Note that H, D, and Z in (2) in general designate some prefiltered field, in order to select a specific frequency band for study.

THE PARKINSON VECTOR

The work of *Parkinson* [1959, 1962*a*, *b*, 1964] resulted in the fact that the plane polarization of geomagnetic disturbances became well recognized and well known in the scientific world. Parkinson's analysis proceeded as follows. Consider (1) and write the unit vector

$$\mathbf{w}(t, \Delta t) = \mathbf{W}(t, \Delta t)/|\mathbf{W}(t, \Delta t)| \tag{3}$$

Then for a set of data filtered by the Parkinson's filter with the time increment Δt the points of each unit vector are plotted in three-dimensional spherical coordinates. By definition the set of points $\mathbf{w}(t, \Delta t)$ will all lie on a spherical surface of unit radius.

Different methods can be used for representing the spherical distribution. *Parkinson* [1959, 1962*a*, *b*, 1964] used an orthographic projection. That is, the unit sphere is observed from infinity. Parkinson separately plotted the upper and lower portions of the spherical surface projected onto the plane: the upper half of the unit sphere is seen from infinity from above, and the lower half is seen from infinity from below. This procedure results in a 'Parkinson plot' [*Parkinson*, 1959, 1962*a*, *b*, 1964]. Examples of Parkinson plots have been reported in numerous papers [e.g., *Price*, 1967].

Other projections of the unit sphere distribution have been suggested. For instance, *Lajoie and Caner* [1970] and *Caner et al.* [1971] used a Mercator projection. *Simeon and Sposito* [1968] suggested using a gnomonic projection (that is, a projection whereby the spherical surface is projected from its center onto a flat plane tangent to the sphere at a point on the equator).

Independent of whichever projection is used, it is found that the points on the unit sphere are not distributed uniformly: in general, the points tend to be distributed along a plane. Parkinson called the plane in which the variations (for a given frequency) are polarized the 'preferred plane.' *Untiedt* [1964] called this plane the 'plane of reference.' For future reference we can express the equation of this Parkinson plane as

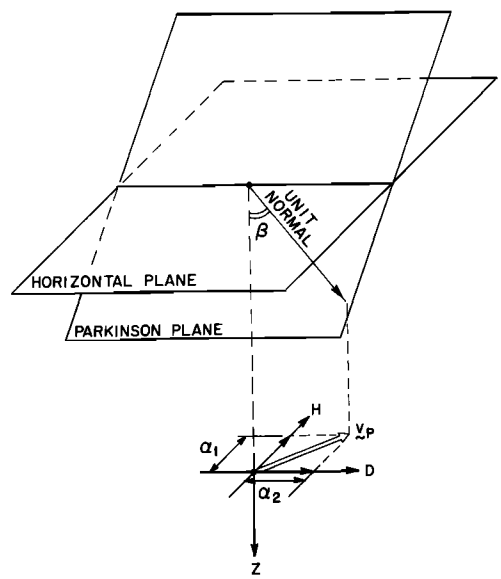

Fig. 2. Definition of the Parkinson vector $\mathbf{v}_P$.

$$\alpha_1 H + \alpha_2 D + \alpha_3 Z = 0 \tag{4}$$

where α_1, α_2, and α_3 are direction cosines.

The concept of an induction arrow, or an induction vector, was introduced by *Parkinson* [1962*a*]. This vector is defined by projecting the downward unit normal to the Parkinson plane onto the horizontal plane. If β is the tilt of the Parkinson plane with respect to the horizontal plane, then the length of the Parkinson vector $\mathbf{v}_P$ is given (see Figure 2) by

$$|\mathbf{v}_P| = \sin \beta \tag{5}$$

Since Z is oriented downward, perpendicular to the horizontal plane, the Parkinson vector has components which are two direction cosines of the Parkinson plane, namely, α_1 along the H axis and α_2 along the D axis. These definitions are illustrated in Figure 2.

THE WIESE VECTOR

Wiese [1962] introduced a different plot in order to investigate the relationship of the horizontal components to the vertical component. We here call this the 'Wiese plot' (see also *Wiese* [1965], *Untiedt* [1964, 1970], *Meyer* [1968], and *Ritter* [1975]). *Wiese* [1962] formally plotted in two dimensions the ratios D/Z as a function of the ratios H/Z. He found that the points (for a given frequency) lay approximately along a straight line, which we call the 'Wiese line.' (We note that *Meyer* [1968] introduces two types of Wiese vectors (see below) in his considerations of possible anomalies produced by a finite conductivity structure underground. This is not necessary in the case of the actual earth, where, for any given frequency, there exists a depth below the finite structure at which the conductivity is infinite so that a Parkinson plane always exists for each frequency at each geographic site.)

We should note that the suggestion for the Wiese plot was obtained from the work of *Constantinescu* [1950], who studied magnetic sudden commencements recorded at Surlari. *Constantinescu* [1950] plotted the azimuthal versus the horizontal variations and drew isolines of constant Z through the plotted points.

That a Wiese line should exist arises from the fact that the magnetic field variation (at a given frequency) lies in the Parkinson plane. This can be seen from the following: Cut the Parkinson plane given by (4) by a plane parallel to the horizontal plane at $Z = 1$. The intersection of these two planes is a line that can be expressed as

$$\frac{\alpha_1}{\alpha_3}\frac{H}{Z} + \frac{\alpha_2}{\alpha_3}\frac{D}{Z} + 1 = 0 \tag{6}$$

This is the form of the Wiese line in the D/Z-H/Z plane.

For the case of the Parkinson plane nearly parallel to the horizontal plane the Wiese line given by (6) is essentially undefined. The Wiese analysis is symmetric in H, D, Z so that, in such a case, the Wiese line can be obtained by cutting the Parkinson plane with a plane at $D = 1$ or $H = 1$ rather than at $Z = 1$.

The equation of the Wiese line (equation (6)) can be rewritten as

$$-r\frac{H}{Z} - y\frac{D}{Z} + 1 = 0 \tag{7}$$

or

$$Z = rH + yD \tag{8}$$

This expression is identical to the Rikitake-Yokoyama relationship (equation (2)), where r and y are given via the direction cosines by $-\alpha_1/\alpha_3$ and $-\alpha_2/\alpha_3$, respectively.

Wiese [1962] defined an induction arrow for his particular geometrical representation as well. He took his arrow to be given by a vector with components $+r$ along the positive H direction and $+y$ along the positive D direction. We call this the 'Wiese vector' $\mathbf{v}_W$.

Now, to find the relationship between the Wiese vector and the 'Parkinson vector,' we note that in the previous section we have shown that the components of the Parkinson vector are given by the directional cosines of the Parkinson plane $+\alpha_1$ and $+\alpha_2$. Hence using (6) and (7), it follows that the Wiese vector is oppositely directed to the Parkinson vector. Moreover, the length of the Wiese vector $|\mathbf{v}_W|$ is given by

$$|\mathbf{v}_W| = (r^2 + y^2)^{1/2} = \left(\frac{1 - \alpha_3^2}{\alpha_3^2}\right)^{1/2} = \left(\frac{\sin^2 \beta}{\cos^2 \beta}\right)^{1/2} = \tan \beta \tag{9}$$

The Parkinson vector $\mathbf{v}_P$ and the Wiese vector $\mathbf{v}_W$ can be written in terms of one another by the expressions

$$|\mathbf{v}_P| = \frac{|\mathbf{v}_W|}{(1 + |\mathbf{v}_W|^2)^{1/2}} \tag{10a}$$

$$|\mathbf{v}_W| = \frac{|\mathbf{v}_P|}{(1 - |\mathbf{v}_P|^2)^{1/2}} \tag{10b}$$

The Wiese plot has been used in a large number of investigations. Normally, the periods considered have ranged from several minutes to several hours. In addition, *Yoshimatsu* [1965] constructed Wiese plots for magnetic pulsations in the period range 15–90 s. He found excellent Wiese lines for the longer periods; for the shorter periods a considerable scatter was obtained, possibly because of the wide 'filter' band used. *Kopyitenko et al.* [1967] found excellent Wiese lines in data ($T \sim 20$ s, 45 s, 70 s, and 45 min) taken in Kamchatka.

THE SCHMUCKER VECTOR

Schmucker [1964, 1970*a*, *b*] introduced the transfer function technique (see also *Everett and Hyndman* [1967]). A complete review and discussion of this procedure is given in a paper in preparation. For our present purposes it is sufficient to note that the starting point for the transfer function technique is the Rikitake-Yokoyama relationship (equation (3)). However, Schmucker uses both the magnitude and phase relationships and thus has both a real part and an imaginary part in his analysis. The real parts of the induction transfer function give rise to an 'in-phase' induction arrow, and the imaginary parts to an 'out-of-phase' (or 'quadrature') induction arrow. For our present concern we consider only the in-phase induction arrow, which can be called the 'Schmucker vector.' The Schmucker vector $\mathbf{v}_S$ is defined with reference to (8), taking $-r$ along the positive H and $-y$ along the positive D direction. That is,

$$\mathbf{v}_S = -\mathbf{v}_W \tag{11}$$

and $\mathbf{v}_S$ is in the same direction as $\mathbf{v}_P$. Other relationships between the Schmucker vector and the Parkinson vector can be derived using (10) and (11).

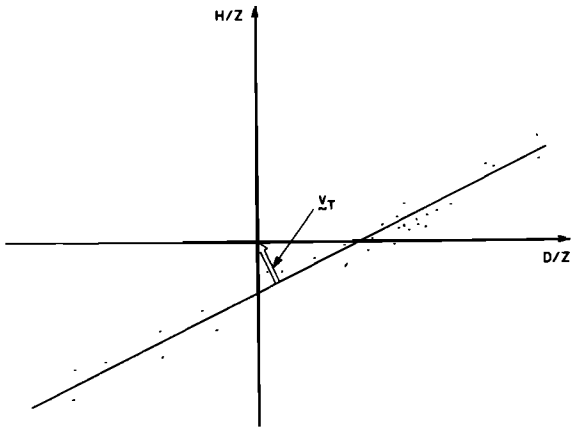

Fig. 3. Definition of the Porath vector $\mathbf{v}_T$ from a Wiese plot.

THE PORATH VECTOR

Porath [1970] and *Porath and Dziewonski* [1971] proposed that an induction vector $\mathbf{v}_T$ could be defined by the vector (length and direction) consisting of the normal projected from the Wiese line and intersecting the origin of the H/Z-D/Z plane. The definition of the Porath vector is illustrated in Figure 3. In order to obtain the relationship between the Porath vector $\mathbf{v}_T$ and $\mathbf{v}_P$, $\mathbf{v}_S$, $\mathbf{v}_W$, write (8) in its normal form

$$\frac{r}{(r^2+y^2)^{1/2}}\frac{H}{Z}+\frac{y}{(r^2+y^2)}\frac{D}{Z}=\frac{1}{(r^2+y^2)^{1/2}} \tag{12}$$

Then the normal to the Wiese line through the origin has the direction cosines $+r/(r^2+y^2)^{1/2}$ and $+y/(r^2+y^2)^{1/2}$. Obviously, because of the sign of these two direction cosines, $\mathbf{v}_T$ has a direction identical to that of $\mathbf{v}_W$, as *Porath* [1970] and *Porath and Dziewonski* [1971] noted. The length of the Porath vector is given as

$$|\mathbf{v}_T|=\frac{1}{(r^2+y^2)^{1/2}}=\frac{1}{|\mathbf{v}_W|} \tag{13}$$

THE YOKOYAMA PLOT

In the previous sections, three methods of construction of induction arrows have been reviewed, and the interrelationships among them have been described. In addition, the relationship of the Schmucker vector (the in-phase induction arrow) to the Parkinson vector was pointed out.

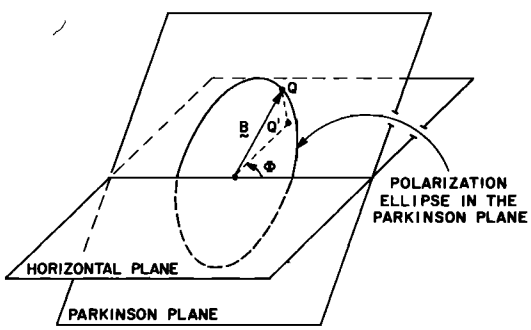

Fig. 4. Definition of the azimuthal direction Φ in the horizontal plane. The point Q lies on the polarization ellipse in the Parkinson plane.

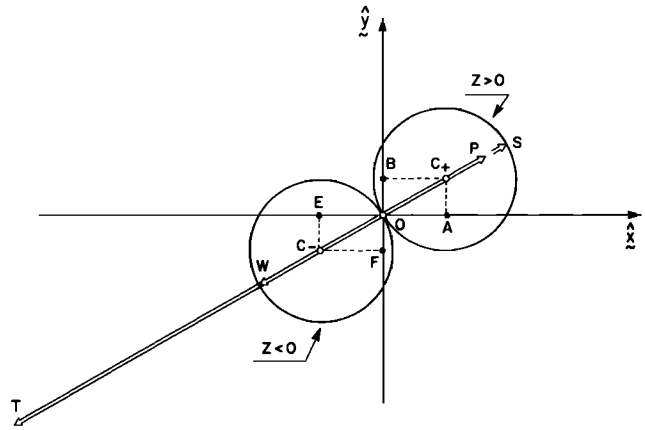

Fig. 5. Schematic illustration of a Yokoyama plot in the horizontal (H-D) plane. The circle of points with $Z > 0$ has a center at C_+; the circle of points with $Z < 0$ has a center at C_-. The Parkinson vector $\mathbf{v}_P$ equals the line **OP**, the Schmucker vector $\mathbf{v}_S$ = **OS**, the Wiese vector $\mathbf{v}_W$ = **OW**, and the Porath vector $\mathbf{v}_T$ = **OT**. The Rikitake-Yokoyama constants are given by $r/2 = |\overline{EO}| = |\overline{OA}|$, $y/2 = |OB| = |\overline{OF}|$, and $r_Y = |\overline{OC_+}| = |\overline{OC_-}|$.

Consider now Figure 4. The time variation of the magnetic field traces a polarization ellipse in the Parkinson plane. Consider a point Q on the ellipse; project it onto the horizontal plane to point Q'. In the horizontal plane an azimuthal angle Φ can specify the direction of the line OQ' with respect to some preselected reference direction. Since Φ is specified by the instantaneous values of H and D, a plot of Z (the length $\overline{QQ'}$) versus Φ will result in a sinusoidal trend. Call Φ_0 the azimuth of maximum correlation between the horizontal field $\mathbf{R}$ ($|\mathbf{R}| = (H^2+D^2)^{1/2}$, direction being given by $\tan^{-1}(H/D)$) and the vertical field Z. From spherical trigonometry,

$$Z=|\mathbf{R}(\Phi)|\tan\beta\cos(\Phi-\Phi_0) \tag{14}$$

This relationship has been verified experimentally by *Voppel* [1964], *Livingstone* [1967], *Fanselau and Treumann* [1968], *Lajoie and Caner* [1970], and *Caner et al.* [1971], as well as by *Banks* [1975], who used a more involved method and found considerable scatter in his plot of $Z/|R(\Phi)|$ versus Φ. In practice, such checks of (14) are Mercator projections of Parkinson plots (see above).

A very interesting geometric representation of geomagnetic signals was proposed by *Yokoyama* [1961, 1962]. It develops from an analysis of what we call the 'Yokoyama plot.' Yokoyama plots have been used by *Giorgi and Yokoyama* [1967, 1968] in studying geomagnetic fluctuations in Sardinia. To define the Yokoyama representation for each of the points on the polarization ellipse (see Figure 4), define a vector in the Φ direction with a length given as

$$I=\frac{Z}{(H^2+D^2)^{1/2}} \tag{15}$$

Then draw, in the H-D (horizontal) plane, the locus of all points given by this vector. Note that the sign of I is determined by the sign of Z. Analytically, the direction of such a vector in the horizontal plane is given by the components

$$X=\text{const}\cdot H \tag{16a}$$

$$Y=\text{const}\cdot D \tag{16b}$$

where $\hat{x}$ is the axis along the positive H direction and $\hat{y}$ is the axis along the positive D direction (see Figure 5). The constant follows from condition (15); i.e.,

$$\text{const} = \frac{Z}{(H^2 + D^2)} \tag{16c}$$

Now, $H(t)$, $D(t)$, and $Z(t)$ all lie in the Parkinson plane and satisfy the Rikitake-Yokoyama relationship (2). Thus using (2), (15), and (16), we find by simple algebra that

$$X^2 + Y^2 = \pm(rX + yY) \tag{17}$$

Thus the coordinates X and Y represent two circles which we call the 'Yokoyama circles.' It can easily be verified that the circles are tangent to each other at the origin (see Figure 5). The circles have centers located at

$$C_+ = \left(\frac{r}{2}, \frac{y}{2}\right) \tag{18a}$$

$$C_- = \left(\frac{-r}{2}, \frac{-y}{2}\right) \tag{18b}$$

with a radius (which we call the 'Yokoyama radius') given by

$$r_Y = \tfrac{1}{2}(r^2 + y^2)^{1/2} \tag{19}$$

One of the circles contains the points with $Z > 0$ (that is, one half of the polarization ellipse in the Parkinson plane), and the other circle contains the points with $Z < 0$ (that is, the other half of the polarization ellipse in the Parkinson plane).

Now, using (9) and (10), the relationship between the magnitude of the Wiese vector $|\mathbf{v}_W|$ and the Yokoyama radius is easily found:

$$|\mathbf{v}_W| = 2r_Y \tag{20}$$

Thus $\mathbf{v}_S$ is the diameter of the circle with the $Z > 0$ points and is oriented from the origin in the positive direction. The Wiese vector $\mathbf{v}_W$ is the same but for the set of points with $Z < 0$. The relationships between the Yokoyama plot and the previously discussed vectors is illustrated in Figure 5, as are the relationships to the Rikitake-Yokoyama constants.

The great utility of the Yokoyama plot can be summarized in the following way. In practice, there will be some scattering of the I values (equation (15)) in the H-D plane. After plotting the I values the barycenters of the plotted points with $Z > 0$ (C_+) and with $Z < 0$ (C_-) could be found separately. The Schmucker vector $\mathbf{v}_S$ (direction and magnitude) is then obtained immediately, with no computation, by the vector directed from C_- to C_+. (This vector should also cross the origin, providing a check on the statistical reliability of the plotted data.)

A Yokoyama plot can also be easily formed, using the symmetry of the two circles and their tangency at the origin. That is, for all points with $Z < 0$, invert the signs of all three components (H, D, and Z) and plot each point as a $Z > 0$ point. The line from the origin to the barycenter C_+ gives the direction and half the length of the Schmucker vector $\mathbf{v}_S$. This procedure appears to be the most straightforward method of determining an induction vector.

For the sake of completeness we should also note that *Berdichevskiy* [1968] and *Berdichevskiy and Smirnov* [1971], in an independent derivation of the Yokoyama plot, proposed a version which took into account possible phase variations. That is, these authors proposed to plot, as a function of the angular direction Φ, not only the magnitude of the ratio (15) (as is done for the Yokoyama plot) but also its phase. In order to define a phase the denominator in (15) should be substituted by an expression such as

$$|A_1 e^{(i\omega t + \gamma_1)}\hat{x} + A_2 e^{(i\omega t + \gamma_2)}\hat{y}| \tag{21}$$

where A_1, A_2, γ_1, and γ_2 are real constants. The choice of (21) is equivalent to not changing the denominator in (15). In this case the phase of (15) is the phase of Z, or of $(\omega t + \gamma_3)$, where γ_3 is a real constant. In such a case the polar diagram of arg I plotted versus Φ or versus t becomes a spiral, as *Berdichevskiy* [1968] and *Berdichevskiy and Smirnov* [1971] state.

However, equivalent to (21) we can write as the denominator of (15)

$$e^{(i\omega t + \psi)}|A_1 e^{\gamma_1}\hat{x} + A_2 e^{\gamma_2}\hat{y}| \tag{22}$$

with ψ an arbitary but fixed constant. In this case the phase of (15) will be a constant, and the polar diagram becomes a circle. Hence the polar diagram of the phase of (15) is indicative at most of the goodness of the filter used in processing the original geomagnetic data. However, no new physical understanding is given by such a technique.

THE WILHJELM ELLIPSOID

Wilhjelm [1968] proposed a very interesting method for evaluating the geomagnetic depth sounding parameters (i.e., the elements by which any induction arrow can be evaluated). For a given frequency the geomagnetic parameters H, D, and Z are plotted in a three-dimensional space. Wilhjelm assumed that the point distribution in the three-dimensional space of the geomagnetic variations has its barycenter at the origin. This is equivalent to assuming that the total time interval of data recording is equal to an integer number of cycles around the polarization ellipse in the Parkinson plane. Whenever this assumption does not hold, it is desirable, for mathematical rigor, to displace the origin to the actual barycenter of the point distribution. However, for actual geophysical applications it is more desirable to assume that the barycenter of the points in the three-dimensional distribution lies at the origin of the three-dimensional coordinate system, even if it is necessary to change, in a suitable way, the total time interval of recordings used.

Now, consider an arbitrary plane (Ω) through the origin having direction cosines ι_1, ι_2, ι_3. Call $\hat{u}$ the unit vector normal to this arbitrary plane (i.e., $\hat{u} = \iota_1, \iota_2, \iota_3$). Define the second-order moment of the point distribution associated with the given direction $\hat{u}$:

$$\mu_{\hat{u}} = \frac{1}{N-1}(\Sigma \hat{u} \cdot \mathbf{B})^2 \tag{23}$$

where N is the total number of points in the three-dimensional distribution. Call

$$\sigma_{\hat{u}} = (\mu_{\hat{u}})^{1/2} \tag{24}$$

the standard deviation of the distance of the points from the plane Ω. Write (23) in the form

$$\mu_{\hat{u}} = \sum_{i,j=1}^{3} \mu_{ij}\iota_i\iota_j \tag{25a}$$

where

$$\mu_{ij} = \frac{1}{N-1}\Sigma B_i B_j \tag{25b}$$

$$\sum_{i,j=1}^{3} \mu_{ij} X_i X_j = 1 \qquad (25c)$$

where $X_i = \iota_i/\sigma_{\hat{u}}$. Equation (25*c*) represents an ellipsoid because, by definition in (25*a*), $\mu_{\hat{u}}$ is always positive. It is the ellipsoid spanned by the locus of the points which, in each given direction $\hat{\mathbf{u}}$, are at a distance $1/\sigma_{\hat{u}}$ from the center.

Wilhjelm [1968] called (25*c*) the 'magnetic activity ellipsoid'; we call it the 'Wilhjelm ellipsoid.' The properties in (25) are not specific to the geomagnetic field but hold for any vector field. That is, the tensor μ_{ij} (equation (25*b*)) is symmetric, and (25*a*) is the invariant quadratic form associated with it. Since we use a three-dimensional space, such a quadratic form is actually an invariant quadratic.

The Wilhjelm ellipsoid (equation (25*c*)) can be reduced to its canonical axes (in terms of a reference frame defined by the unit vectors $\hat{\mathbf{x}}_1'$, $\hat{\mathbf{x}}_2'$, $\hat{\mathbf{x}}_3'$):

$$\left(\frac{X_1'}{a}\right)^2 + \left(\frac{X_2'}{b}\right)^2 + \left(\frac{X_3'}{c}\right)^2 = 1 \qquad (26)$$

where we have assumed that $a \geq b \geq c$.

Finally, notice that a perfectly plane-polarized field $\mathbf{B}(t)$ means that $\sigma_{\hat{u}} = 0$ along the direction perpendicular to the Parkinson plane. In such a case, a in (26) goes to infinity. Or, in other words, the normal to the Parkinson plane has the same directional cosines as the $\hat{\mathbf{x}}_1'$ axis. These direction cosines are those used above in the discussion of the Parkinson plane.

CONCLUSION

We have reviewed the following induction arrows (or induction vectors): (1) the Parkinson vector $\mathbf{v}_P$, (2) the Wiese vector $\mathbf{v}_W$, (3) the Schmucker vector $\mathbf{v}_S$, and (4) the Porath vector $\mathbf{v}_T$. The vectors can be derived by using any one of the following tools: (1) the Parkinson plot, (2) the Wiese plot, (3) the Porath method, (4) the Yokoyama plot, and (5) the Wilhjelm ellipsoid. This review has shown that all of the vectors can be related to one another; one is not 'better' than another. The Yokoyama plot provides the unification of the various methodologies and is the most straightforward means for deriving the vectors. The generalization of the Yokoyama plot proposed by *Berdichevskiy* [1968] and *Berdichevskiy and Smirnov* [1971] does not provide additional information.

An intrinsic limitation of these approaches lies in the fact that all such methods are essentially based on the Rikitake-Yokoyama relationship (2), with real coefficients r and y. Considerations of complex Rikitake-Yokoyama constants r and y necessarily imply a full discussion of the transfer function technique, a technique formally introduced by *Schmucker* [1964, 1970*a*, *b*] and discussed also by *Everett and Hyndman* [1967]. A full discussion of this technique is reviewed in a paper in preparation.

Finally, we note that occasionally, in an application, one of the vectors discussed herein is rotated by 90° in order to represent the 'equivalent current' direction of the anomalous field responsible for the vector [e.g., *Fanselau and Treumann*, 1966; *Schmucker*, 1970*a*]. In this case, *Lilley* [1976] pointed out that the length of the vector should be scaled by the factor $\tan^{-1}(H^2 + D^2)^{1/2}/Z$ (i.e., by $\tan^{-1}|\mathbf{v}_T|$, by $\tan^{-1}|1/\mathbf{v}_S|$, or by $\tan^{-1}|1/\mathbf{v}_W|$). As he also noted, the vector would appear with a maximum length directly above the conductor responsible for the anomaly.

NOTATION

- a longest axis of the Wilhjelm ellipsoid.
- A A_1, A_2, A_3: amplitudes of the three components of the observed geomagnetic field at a given frequency ν.
- b intermediate axis of the Wilhjelm ellipsoid.
- $\mathbf{B}(t)$ geomagnetic field, prefiltered within some given frequency band $\Delta\nu$.
- c the shortest axis of the Wilhjelm ellipsoid.
- D west-east component of $\mathbf{B}(t)$.
- H south-north component of $\mathbf{B}(t)$.
- i imaginary unit.
- i tensorial index.
- I ratio $Z/(H^2 + D^2)^{1/2}$.
- j tensorial index.
- N total number of points in the Wilhjelm three-dimensional plot.
- P subscript; $\mathbf{v}_P$ is the Parkinson vector.
- r first Rikitake-Yokoyama constant.
- r_Y Yokoyama radius.
- $\mathbf{R}$ two-dimensional vector lying in the horizontal plane having components H and D.
- S subscript; $\mathbf{v}_S$ is the Schmucker vector.
- t time.
- T subscript; $\mathbf{v}_T$ is the Porath vector.
- $\hat{\mathbf{u}}$ unit vector of components ι_1, ι_2, ι_3.
- $\mathbf{v}$ induction vector or induction arrow.
- $\mathbf{w} = \mathbf{w}(t, \Delta t) = \mathbf{W}(t, \Delta t)/|\mathbf{W}(t, \Delta t)|$.
- $\mathbf{W} = \mathbf{W}(t, \Delta t) = \mathbf{B}(t + \Delta t) - \mathbf{B}(t)$.
- W subscript; $\mathbf{v}_W$ is the Wiese vector.
- x x axis; $\hat{\mathbf{x}}$ is unit vector along it.
- X component along $\hat{\mathbf{x}}$.
- x $\hat{\mathbf{x}}_1'$, $\hat{\mathbf{x}}_2'$, $\hat{\mathbf{x}}_3'$, alternative coordinate system (reducing the Wilhjelm ellipsoid to its canonical form).
- X' component along $\hat{\mathbf{x}}'$.
- y y axis; $\hat{\mathbf{y}}$ is unit vector along it.
- y second Rikitake-Yokoyama constant.
- Y component along $\hat{y}$.
- Z vertical component of $\mathbf{B}(t)$.
- α α_1, α_2, α_3, direction cosines of the Parkinson plane.
- β tilt angle of the Parkinson plane with the horizontal plane.
- γ γ_1, γ_2, γ_3, phases of the three components of the observed geomagnetic field $\mathbf{B}(t)$ at some given frequency ν.
- Δ variation of a quantity between two different time instants or within some limited interval.
- ι ι_1, ι_2, ι_3, directional cosines of Ω.
- $\mu_{\hat{u}} = \sigma_{\hat{u}}^{-2}$.
- μ_{ij} tensor.
- ν frequency.
- $\sigma_{\hat{u}}$ standard deviation (in deriving the Wilhjelm plot).
- Φ angle.
- ψ phase.
- ω angular speed.
- Ω arbitrary plane.

REFERENCES

Babour, K., and J. Mosnier, Differential geomagnetic sounding, *Geophysics, 42*, 66, 1977.

Babour, K., J. Mosnier, M. Daignieres, G. Vasseur, J. L. LeMouël, and J. C. Rossignol, A geomagnetic variation anomaly in the northern Pyrenees, *Geophys. J. Roy. Astron. Soc., 45*, 583, 1976.

Bailey, R. C., Inversion of the geomagnetic induction problem, *Proc. Roy. Soc., Ser. A, 315,* 185, 1970.

Baird, H. F., A preliminary investigation of some features of four magnetic storms recorded at seven magnetic observatories in the Pacific Ocean region during 1924, Ph.D. thesis, Univ. of New Zealand, Wellington, 1927.

Banks, R. J., Complex demodulation of geomagnetic data and the estimation of transfer functions, *Geophys. J. Roy. Astron. Soc., 43,* 87, 1975.

Berdichevskiy, M. N., *Electrical Prospecting by the Method of Magnetotelluric Profiling* (in Russian), Nedra, Moscow, 1968.

Berdichevskiy, M. N., and V. S. Smirnov, Methods of analyzing observations during magnetic variation profiling, *Geomagn. Aeron., 11,* 310, 1971.

Berdichevskiy, M. N., E. B. Fainberg, N. M. Rotanova, J. B. Smirnov, and L. L. Vanyan, Deep electromagnetic investigations, *Ann. Geophys., 32,* 143, 1976.

Bossolasco, M., Sur la nature des perturbations magnétiques, *C. R. Acad. Sci., 203,* 676, 1936.

Caner, B., D. R. Auld, H. Dragert, and P. A. Camfield, Geomagnetic depth-sounding and crustal structure in western Canada, *J. Geophys. Res., 76,* 7181, 1971.

Constantinescu, L., Sudden commencements of magnetic storms in the years 1944–1949 (in Rumanian), *Lucr. Ses. Gen. Stiint. Acad. Rep. Pop. Rom.,* 1950.

Everett, J. E., and R. D. Hyndman, Geomagnetic variations and electrical conductivity structure in southwestern Australia, *Phys. Earth Planet. Interiors, 1,* 24, 1967.

Fanselau, G., The use of range-differences for the interpretation of conductivity anomalies, *Phys. Earth Planet. Interiors, 1,* 177, 1968*a*.

Fanselau, G., Einige Bemerkungen zur kleinregionalen Veränderlichkeit von *Sq, Beitr. Geophys., 77,* 35, 1968*b*.

Fanselau, G., The use of long-period variations for geomagnetic depth-sounding, *Acta Geol. Geophys. Montan. Hung., 5*(1/2), 79, 1970.

Fanselau, G., and R. Treumann, Zur magnetischen Tiefensondierung, *Geofis. Pura Appl., 65,* 54, 1966.

Fanselau, G., and R. Treumann, Untersuchungen zur Interpretation der Ergebnisse geomagnetischer Tiefensondierungen, *Geologie, 17,* 76, 1968.

Fukushima, N., Equivalence in ground geomagnetic effect of Cnapman-Vestine's and Birkeland-Alfvén's electric current systems for polar magnetic storms, *Rep. Ionosph. Space Res. Japan, 23,* 219, 1969.

Fukushima, N., Remarks on plasmapause and current systems, *Handb. Phys., 49,* 103, 1972.

Gauss, C. F., Allgemeine Theorie des Erdmagnetisms, in *Resultate magn. Verein. 1838,* Göttingen and Leipzig, Germany, 1838. (Reprinted in *Werke, 5,* 121–193.)

Giorgi, M., and I. Yokoyama, Geomagnetic variations observed at Maddalena island, Sardinia, *Nature, 214,* 477, 1967.

Giorgi, M., and I. Yokoyama, Anomalies of geomagnetic variations observed at Maddalena island, Sardinia, and their probable causes, *Quad. Ric. Scient., 44,* 22 pp., 1968.

Kopyitenko, Yu. A., E. S. Gorshkov, T. A. Gorshkova, I. S. Fel'dman, and T. A. Fel'dman, Magnetotelluric sounding in the Klyuchi settlement of the Kamchatka region, *Izv. Acad. Sci. USSR Phys. Solid Earth,* 609, 1967.

Lajoie, J. J., and B. Caner, Geomagnetic induction anomaly near Kootenay lake: A strip-like feature in the lower crust?, *Can. J. Earth Sci., 7,* 1568, 1970.

Lilley, F. E. M., A magnetometer array study across southern Victoria and the Bass Straight area, Australia, *Geophys. J. Roy. Astron. Soc., 46,* 165, 1976.

Livingstone, C. E., Geomagnetic depth-sounding in the Southwest USA and in southern British Columbia, M.Sc. thesis, p. 57, Univ. of B. C., Vanouver, 1967.

Meyer, J., Über die Richtungsveranderlichkeit des geomagnetischen Induktionpfeils bei endlicher Leitfähigkeit, *Z. Geophys., 34,* 195, 1968.

Parkinson, W. D., Direction of rapid geomagnetic fluctuations, *Geophys. J. Roy. Astron. Soc., 2,* 1, 1959.

Parkinson, W. D., The influence of continent and oceans on geomagnetic variations, *Geophys. J. Roy. Astron. Soc., 6,* 441, 1962*a*.

Parkinson, W. D., Magnetic variations and the oceans, Geomagnetica, *Publ. 97,* p. 108, Serv. Meteorol. Nac., Lisbon, 1962*b*.

Parkinson, W. D., Conductivity anomalies in Australia and the ocean effect, *J. Geomagn. Geoelec., 15,* 222, 1964.

Porath, H., Determination of strike of conductive structures from geomagnetic variation anomalies, *Earth Planet. Sci. Lett., 9,* 29, 1970.

Porath, H., and A. Dziewonski, Crustal resistivity anomalies from geomagnetic deep-sounding studies, *Rev. Geophys. Space Phys., 9,* 891, 1971.

Price, A. T., Electromagnetic induction within the earth, in *Physics of Geomagnetic Phenomena,* edited by S. Matsushita and W. H. Campbell, 235 pp., Academic, New York, 1967.

Rikitake, T., and I. Yokoyama, Anomalous relations between *H* and *Z* components of transient geomagnetic variations, *J. Geomagn. Geoelec., 5,* 59, 1953.

Ritter, E., Results of geoelectromagnetic deep sounding in Europe, *Beitr. Geophys., 84,* 261, 1975.

Schmucker, U., Anomalies of geomagnetic variations in the southwestern United States, *J. Geomagn. Geoelec., 15,* 193, 1964.

Schmucker, U., Anomalies of geomagnetic variations in the southwestern United States, *Bull. 13,* pp. 1–165, Scripps Inst. of Oceanogr., La Jolla, Calif., 1970*a*.

Schmucker, U., An introduction to induction anomalies, *J. Geomagn. Geoelec., 22,* 9, 1970*b*.

Simeon, G., and A. Sposito, Anomalies of the geomagnetic variations in the Ventolene Island, (in Italian), *Ann. Ist. Nav. Napoli, 37,* 275, 1968.

Skey, H. F., Records of the survey of New Zealand, Report for the year 1926–27, *Rep. 4,* p. 42, Magn. Observ., Christchurch, New Zealand, 1928.

Untiedt, J., Über den linearen Zusammenhang zwischen den Komponenten erdmagnetischer Variationen und seine Bedeutung fur die erdmagnetische Tiefensondierung, *Nachr. Akad. Wiss. Goettingen, Math. Phys. Kl., 2,* 1, 1964.

Untiedt, J., Conductivity anomalies in central and southern Europe, *J. Geomagn. Geoelec., 22,* 131, 1970.

Vestine, E. H., On the analysis of surface fields by integrals, 1, *Terr. Magn. Atmos. Elec., 46,* 27, 1941.

Voppel, D., Erdmagnetische Variationen auf ozeanischen Inzeln, *Deut. Hydrogr. Z., 17,* 179, 1964.

Weidelt, P., The inverse problem of geomagnetic induction, *Z. Geophys., 38,* 257, 1972.

Wiese, H., Geomagnetische Tiefentellurik, 2, Die Streichrichtung der Untergrundstrukturen des elektrischen Widerstandes, erschlossen aus geomagnetischen Variationen, *Geofis. Pura Appl., 52,* 83, 1962.

Wiese, H., Geomagnetische Tiefentellurik, *Abh. Geomagn. Inst. Observ. Potsdam-Neimagh, 36,* 1–146, 1965.

Wilhjelm, J., Non-random influence of external sources on a geomagnetic induction anomaly in northern part of Greenland, *Geophys. J. Roy. Astron. Soc., 16,* 259, 1968.

Yamashita, H., and I. Yokoyama, Interpretation of the 'Northeastern Japan anomaly' in electrical conductivity of the upper mantle, *J. Geomagn. Geoelec., 28,* 329, 1976.

Yokoyama, I., Relations between the short period changes in geomagnetism and in telluric currents, *J. Fac. Sci. Hokkaido Univ., Ser. 7, 1,* 331, 1961.

Yokoyama, I., Relations between the short period changes in geomagnetism and in telluric currents, *J. Fac. Sci. Hokkaido Univ., Ser. 7, 1,* 393, 1962.

Yoshimatsu, T., Results of geomagnetic routine observations and earthquakes, IV, Local time changes of $(\Delta Z/\Delta X)$'s of Pc 3–4 and Pi 2 at Kanoya (in Japanese), *Mem. Kakioka Magn. Observ., 12,* 123, 1965.

(Received January 8, 1979;
accepted August 14, 1979.)